SERVO CONTROL OF RF CAVITIES UNDER BEAM LOADING

Alexander Gamp
DESY, Hamburg, Germany

Abstract
I begin by giving a description of the RF generator–cavity–beam coupled system in terms of basic quantities. Taking beam loading and cavity detuning into account, expressions for the cavity impedance as seen by the generator and as seen by the beam are derived. Subsequently methods of beam-loading compensation by cavity detuning, RF feedback and feedforward are described. Finally, a dedicated phase loop for damping synchrotron oscillations is discussed.

1. INTRODUCTION

In modern particle accelerators RF voltages with an extremely large amplitude and frequency range, from a few hundred volts to hundreds of megavolts and from several kilohertz to many gigahertz, are required for particle acceleration and storage.

The RF power needed to satisfy these demands can be generated, for example, by triodes, tetrodes, or klystrons. The Continuous Wave (CW) output power available from some tetrodes used at DESY is 60 kW at 208 MHz and 500–800 kW for the 500 MHz klystrons. Such RF power generators generally deliver RF voltages of only a few kilovolts because their source impedance is small compared with the cavity shunt impedance. For the TeV Energy Superconducting Linear Accelerator (TESLA) project a prototype pulsed L-band Multibeamklystron has delivered up to 10 MW peak power for 0.5 ms long pulses, and at 3 GHz 150 MW were achieved for pulses of 3 μs in length.

Typically, a tetrode has its highest efficiency for a load resistance of less than 1 kΩ ,whereas the cavity shunt impedance usually is of the order of several megaohms. This is the real impedance, which the cavity represents to a generator at the resonant frequency. It must not be confused with ohmic resistances.

Optimum fixed impedance matching between generator and cavity can be easily achieved with a coupling loop in the cavity. There is, however, the complication that the transformed cavity impedance as seen by the generator depends also on the synchronous phase angle and the beam current and is therefore not constant (as we shall show quantitatively). The beam current induces a voltage in the cavity that may become even larger than the one induced by the generator. Owing to the vector addition of these two voltages the generator now sees a cavity that appears to be detuned and unmatched except for the particular value of beam current for which the coupling has been optimized. The reflected power occurring at all other beam currents has to be handled.

In addition, the beam-induced cavity voltage may cause single- or multi-bunch instabilities, since any bunch in the machine may see an important fraction of the cavity voltage induced by itself or from previous bunches. This voltage is given by the product of beam current and cavity impedance as seen by the beam. Minimizing this latter quantity is therefore essential. It is also called beam-loading compensation, and some servo control mechanisms, which can be used to achieve this goal, will be discussed in this lecture.

2. THE COUPLING BETWEEN THE RF GENERATOR, THE CAVITY, AND THE BEAM

For frequencies in the neighbourhood of the fundamental resonance, an RF cavity can be described [1] by an equivalent circuit consisting of an inductance L_2 , a capacitor *C,* and a shunt impedance R_S, as shown in Fig. 1. In practice, L_2 is made up by the cavity walls, whereas the coupling loop L_1 is usually small compared with the cavity dimensions.

In this example a triode with maximum efficiency for a real load impedance R_A has been taken as an RF power generator. For simplicity we consider a short and lossless transmission line between the generator and L_1. Then there is optimum coupling between the generator and the empty (i.e. without beam) cavity for

$$N^2 = R_S / R_A = L_2 / L_1 \ , \tag{1}$$

where R_A equals the dynamic source impedance R_1. The term *N* is the transformation or step-up ratio.

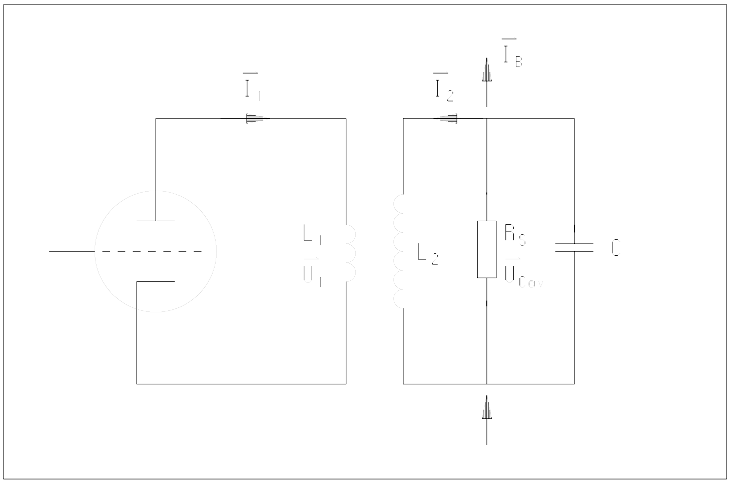

Fig. 1: Equivalent circuit of a resonant cavity near its fundamental resonance. In practice, the inductance L_2 is made up by the cavity walls, whereas L_1 is usually a small coupling loop.

Since, in general, there may be power transmitted from the generator to the cavity and also, in the case of imperfect matching, vice versa, the voltage $\vec{U}_1$ is expressed as the sum of two voltages

$$\vec{U}_1 = \vec{U}_{\text{forward}} + \vec{U}_{\text{reflected}} \ , \tag{2}$$

whereas the corresponding currents flow in the opposite directions, hence

$$\vec{I}_1 = \vec{I}_{\text{forward}} - \vec{I}_{\text{reflected}} \ . \tag{3}$$

The minus sign in Eq. (3) indicates the counterflowing currents, while voltages of forward and backward waves just add up.

So, in the simplest case, where the beam current $\vec{I}_B = 0$ and where the generator frequency $f_{GEN} = f_{CAV}$, there is no reflected power from the cavity to the generator, and $\vec{U}_1$ and $\vec{I}_1$ are identical to the generator voltage and current, respectively. One has

$$\vec{U}_{CAV} = N\vec{U}_1 \ . \tag{4}$$

Now we can derive an expression for the complex cavity voltage as a function of generator and beam current and of the cavity and generator frequency.

According to Fig. 1 the cavity voltage $\vec{U}_{\mathrm{CAV}}$ can be written as

$$\vec{U}_{\mathrm{CAV}} = L_2\left(\frac{\dot{\vec{I}}_2 + \dot{\vec{I}}_1}{N}\right) \tag{5}$$

$$\vec{I}_2 = -\left(\frac{\vec{I}_{\mathrm{B}} + \vec{U}_{\mathrm{CAV}}}{R_{\mathrm{S}} + C\dot{\vec{U}}_{\mathrm{CAV}}}\right). \tag{6}$$

All voltages and currents have the time dependence

$$\vec{U} = \hat{\vec{U}}e^{i\omega t}. \tag{7}$$

$\vec{I}_{\mathrm{B}} = \vec{I}_{\mathrm{B}}(\omega)$ is the harmonic content at the frequency ω of the total beam current. Throughout this lecture we consider only a bunched beam with a small bunch spacing compared to the cavity filling time. In this case $\vec{I}_{\mathrm{B}}(\omega)$ is quasi sinusoidal. We also restrict the discussion to the interaction of the beam with the fundamental cavity resonance. Dedicated damping antennas built into the cavity can minimize the interaction with higher-order cavity modes.

Inserting Eq. (6) in Eq. (5) and using

$$2\pi f_{\mathrm{CAV}} = \omega_{\mathrm{CAV}} = \frac{1}{\sqrt{L_2 C}} \tag{8}$$

one finds

$$\omega_{\mathrm{CAV}}^2\vec{U}_{\mathrm{CAV}} = \frac{1}{C}\left[\frac{1}{N}\dot{\vec{I}}_1 - \dot{\vec{I}}_{\mathrm{B}} - \frac{1}{R_{\mathrm{S}}}\dot{\vec{U}}_{\mathrm{CAV}}\right] - \ddot{\vec{U}}_{\mathrm{CAV}} . \tag{9}$$

We define

$$\Gamma = \frac{1}{2CR_{\mathrm{S}}} = \frac{\omega_{\mathrm{CAV}}}{2Q} \tag{10}$$

where the quality factor of the cavity can be expressed as 2π times the ratio of total electromagnetic energy stored in the cavity to the energy loss per cycle.

Here we would like to mention that the ratio

$$\frac{R_{\mathrm{S}}}{Q} = \sqrt{\frac{L_2}{C}} \tag{11}$$

is a characteristic quantity of a cavity depending only on its geometry.

We can rewrite Eq. (9) as

$$\ddot{\vec{U}}_{\mathrm{CAV}} + 2\Gamma\dot{\vec{U}}_{\mathrm{CAV}} + \omega_{\mathrm{CAV}}^2\vec{U}_{\mathrm{CAV}} = 2\Gamma R_{\mathrm{S}}\left[\frac{1}{N}\dot{\vec{I}}_1 - \dot{\vec{I}}_{\mathrm{B}}\right] . \tag{12}$$

This equation describes a resonant circuit excited by the current $\vec{I} = \left(\vec{I}_1\big/\left(N - \vec{I}_{\mathrm{B}}\right)\right)$. The minus sign occurs because the generator-induced cavity voltage has opposite sign to the beam-induced voltage, which would decelerate the beam. It can be shown that the beam actually sees only 50% of its own induced voltage. This is called the fundamental theorem of beam loading [2, 3].

In order to find the cavity impedance as seen by the beam we make use of Eqs. (2), (3), and (4) to express the generator current term of Eq. (12) in the form

$$\frac{1}{N}\dot{\vec{I}}_1 = \frac{1}{NR_\mathrm{A}}\left[2\dot{\vec{U}}_\mathrm{forward} - \dot{\vec{U}}_1\right] = \frac{1}{N}\left[2\dot{\vec{I}}_\mathrm{forward} - \frac{\dot{\vec{U}}_\mathrm{CAV}}{NR_\mathrm{A}}\right] \quad . \tag{13}$$

This leads to a modification of the damping term in Eq. (12)

$$\ddot{\vec{U}}_\mathrm{CAV} + 2\Gamma(1+\beta)\dot{\vec{U}}_\mathrm{CAV} + \omega_\mathrm{CAV}^2\vec{U}_\mathrm{CAV} = 2\Gamma_\mathrm{L}R_\mathrm{SL}\left[\frac{2}{N}\dot{\vec{I}}_\mathrm{f} - \dot{\vec{I}}_\mathrm{B}\right] \quad . \tag{14}$$

With the coupling ratio

$$\beta = R_\mathrm{S}/\left(N^2 R_\mathrm{I}\right) \tag{15}$$

we can introduce the 'loaded' damping term

$$\Gamma_\mathrm{L} = \Gamma(1+\beta) \tag{16}$$

and consequently, in accordance with Eq. (10), the loaded cavity Q and loaded shunt impedance are

$$Q_\mathrm{L} = Q/(1+\beta) \quad \text{and} \quad R_\mathrm{SL} = R_\mathrm{S}/(1+\beta) \ . \tag{17}$$

In the case of perfect matching in the absence of beam, i.e. $\beta = 1$, the damping term simply doubles and Q and R_S take half their original values. This is because the beam would see the cavity shunt impedance R_S in parallel or loaded with the transformed generator impedance $N^2R_\mathrm{I} = R_\mathrm{S}$. Therefore we find in Eq. (14) that the transformed generator current

$$\vec{I}_\mathrm{G} = 2\vec{I}_\mathrm{f}/N \tag{18}$$

gives rise to twice as much cavity voltage as a similar beam current would do. Here and in Eq. (15) we assume that the transformed dynamic source impedance N^2R_I is identical to the generator impedance seen by the cavity. This is strictly true only if a circulator is placed between the RF power generator and the cavity. Without a circulator it may be approximately true if the power source is a triode. Owing to its almost constant anode-voltage-to-current characteristic the impedance of a tetrode as seen from the cavity is, however, much bigger than the corresponding R_I and therefore $R_\mathrm{SL} \approx R_\mathrm{S}$ here, where a short transmission line (or of length $n\lambda/2$, n integer) is considered.

Following Ref. [4] we write the solution of Eq. (14) in the Fourier–Laplace representation

$$\hat{\vec{U}}_\mathrm{CAV} = \frac{i\omega}{\omega_\mathrm{CAV}^2 - \omega^2 + 2i\omega\Gamma_\mathrm{L}} 2\Gamma_\mathrm{L}R_\mathrm{SL}\left[\hat{\vec{I}}_\mathrm{G} - \hat{\vec{I}}_\mathrm{B}\right] \ . \tag{19}$$

For $\Delta\omega \cdot \omega_\mathrm{CAV}$ this can be approximated by

$$\hat{\vec{U}}_\mathrm{CAV} \approx \frac{R_\mathrm{SL}\left[\hat{\vec{I}}_\mathrm{G} - \hat{\vec{I}}_\mathrm{B}\right]}{1 + iQ_\mathrm{L}2\dfrac{\Delta\omega}{\omega_\mathrm{CAV}}} \quad , \tag{20}$$

where $\omega = \omega_\mathrm{CAV} + \Delta\omega$.

For a resonant cavity the beam-induced voltage $\vec{U}_\mathrm{B}$, or the beam loading, is thus given by the product of loaded shunt impedance and beam current:

$$\vec{U}_{\mathrm{B}} = -R_{\mathrm{SL}} \vec{I}_{\mathrm{B}} \tag{21}$$

The ideal beam loading compensation would, therefore, minimize R_{SL} without increasing the generator power necessary to maintain the cavity voltage.

Having just discussed the impedance that the combined system generator and cavity represents to the beam, we would like to discuss the impedance Z, or rather admittance $Y = 1/Z$, which the combined cavity and beam system represents to the generator.

From Eqs. (1), (5), and (6) one sees [5] that

$$Y = \frac{\vec{I}_1}{\vec{U}_1} = \frac{N^2}{R_{\mathrm{S}}} + \frac{\vec{I}_{\mathrm{B}} N^2}{\vec{U}_{\mathrm{CAV}}} + \frac{N^2}{i\omega L_2}\left(1 - \frac{\omega^2}{\omega_{\mathrm{CAV}}^2}\right) . \tag{22}$$

which reduces to $Y = 1/R_{\mathrm{A}}$ for a tuned cavity without beam current in the case of $\beta = 1$.

As we are now going to show, a non-vanishing real part of the quotient $\vec{I}_{\mathrm{B}} / \vec{U}_{\mathrm{CAV}}$ will necessitate a change in β to maintain optimum matching, whereas the imaginary part can be compensated by detuning the cavity. In order to work out Re and $\mathrm{Im}(\vec{I}_{\mathrm{B}}/\vec{U}_{\mathrm{CAV}})$, we define the angle ϕ_{s} as the phase angle between the synchronous particle and the zero crossing of the RF cavity voltage. The accelerating voltage is therefore given by

$$\vec{U}_{\mathrm{ACC}} = \vec{U}_{\mathrm{CAV}} \sin\phi_{\mathrm{s}} \tag{23}$$

and the normalized cavity voltage and beam current are related by

$$\frac{\vec{I}_{\mathrm{B}}}{|\vec{I}_{\mathrm{B}}|} = \frac{\vec{U}_{\mathrm{CAV}}}{|\vec{U}_{\mathrm{CAV}}|} e^{\mathrm{i}\left(\frac{\pi}{2} - \phi_{\mathrm{s}}\right)} . \tag{24}$$

Consequently

$$\mathrm{Re}\left(\frac{\vec{I}_{\mathrm{B}}}{\vec{U}_{\mathrm{CAV}}}\right) = \left|\frac{\vec{I}_{\mathrm{B}}}{\vec{U}_{\mathrm{CAV}}}\right| \sin\phi_{\mathrm{s}} \tag{25}$$

and

$$\mathrm{Im}\left(\frac{\vec{\mathrm{I}}_{\mathrm{B}}}{\vec{\mathrm{U}}_{\mathrm{CAV}}}\right) = \left|\frac{\vec{\mathrm{I}}_{\mathrm{B}}}{\vec{\mathrm{U}}_{\mathrm{CAV}}}\right| \cos\phi_{\mathrm{s}} . \tag{26}$$

The real part of the admittance seen by the generator then becomes

$$\mathrm{Re(Y)} = \frac{\mathrm{N}^2}{\mathrm{R_S}}\left(1 + \frac{\mathrm{R_S}|\vec{\mathrm{I}}_{\mathrm{B}}|}{|\vec{\mathrm{U}}_{\mathrm{CAV}}|}\sin\phi_{\mathrm{s}}\right) . \tag{27}$$

We see that the term in the bracket describes the change of admittance caused by the beam. In order to maintain optimum coupling the coupling ratio β must now take the value

$$\beta = \left(1 + \frac{R_{\mathrm{S}}|\vec{I}_{\mathrm{B}}|}{|\vec{U}_{\mathrm{CAV}}|}\sin\phi_s\right) . \tag{28}$$

This result tells us that the change in the real part of the admittance is proportional to the ratio of RF power delivered to the beam to RF power dissipated in the cavity walls. For circular electron machines, where the considerable amount of energy lost by synchrotron radiation has to be compensated continuously by RF power, values of $\phi_s \geq 30°$ and $\beta \geq 1.2$ are typical for high beam current and normally conducting cavities. A typical set of parameters for this case would be $R_S = 6\,\mathrm{M}\Omega$, $\vec{U}_{CAV} = 1$ MV and $\hat{\vec{I}}_B = 30$ mA. This implies, of course, that for a β that has been optimized for the maximum beam current, there will be reflected generator power for lower beam intensities. If the power source is a klystron, this can be handled by inserting a circulator in the path between generator and cavity or, in the case of a tube, by a sufficiently high plate dissipation power capability.

From the imaginary part of Eq. (22) and from Eq. (26) we find that the apparent cavity detuning caused by the beam current can be compensated by a real cavity detuning (for example, by means of a mechanical plunger cavity tuner) of the amount

$$\frac{\omega}{\omega_{CAV}} = \sqrt{1 - \frac{R_S|\vec{I}_B|}{Q|\vec{U}_{CAV}|}\cos\phi_s} \ . \tag{29}$$

Expanding the square root to first order we find a cavity detuning angle Ψ

$$\tan\Psi \approx \frac{R_{SL}|\vec{I}_B|}{|\vec{U}_{CAV}|}\cos\phi_s \approx -2Q_L\frac{\Delta\omega}{\omega_{CAV}} . \tag{30}$$

This is essentially the ratio between beam-induced and total cavity voltage.

In order to calculate the maximum amount of reflected power seen by the generator as a consequence of beam loading we consider, for $\beta = 1$, a tuned cavity, i.e. $\omega = \omega_{CAV}$. Then, with Eqs. (25) and (26), Eq. (22) reads

$$Y = \frac{1}{R_A}\left[1 + \frac{R_S|\vec{I}_B|}{|\vec{U}_{CAV}|}\sin\phi_s + i\,\frac{R_S|\vec{I}_B|}{|\vec{U}_{CAV}|}\cos\phi_s\right] . \tag{31}$$

Solving for $\vec{U}_{refl.}$ by means of Eqs. (2) and (3) the reflected power $P_{refl.} = |\hat{\vec{U}}_{refl.}|^2 / 2R_I$ becomes

$$P_{refl.} = R_S \hat{\vec{I}}_B^2 / 8 . \tag{32}$$

This corresponds to half of the power given by the beam to the coupled system cavity and generator. The second half of this power is dissipated in the cavity walls. All we found is that two equal resistors in parallel dissipate equal amounts of power. As pointed out above, this is strictly true only if a circulator is placed between the RF power source and the cavity. Nevertheless, the amount of reflected power can be quite impressive. For an average DC beam current of, say 0.1 A, the harmonic current $\hat{\vec{I}}_B(\omega)$ may become up to twice as large. Then, taking $R_S = 8$ MΩ, for example, we find 40 kW of reflected power have to be dissipated.

For a cavity where only the reactive part of the beam loading has been compensated by detuning according to Eq. (30), but $\beta = 1$, the reflected power is given by

$$P_{refl.} = R_S \hat{\vec{I}}_B^2 \sin^2\phi_s / 8 . \tag{33}$$

Summarizing the results of this section we state that the beam sees the cavity shunt impedance in parallel with the transformed generator impedance. The resulting loaded impedance is reduced by the factor $1/(1 + \beta)$. The optimum coupling ratio between generator and cavity depends on the amount of energy taken by the beam out of the RF field. The coupling is usually fixed and optimized for maximum beam current. The amount of cavity detuning necessary for optimum matching, on the other hand, depends on the ratio of beam-induced to total cavity voltage.

3. BEAM-LOADING COMPENSATION BY DETUNING

As we have shown in the previous Section, stationary beam loading can be entirely compensated by detuning the cavity, provided that the synchronous phase angle is small or zero. This is usually the case in proton synchrotrons during storage, where the energy loss due to the emission of synchrotron radiation is negligible. Here, the RF voltage is needed only to keep the bunch length short. Energy ramping also takes place at very small ϕ_s.

In the following we restrict ourselves, for simplicity, to hadron machines. Consequently $\beta = 1$, $\phi_s \approx 0$, and the generator- and beam-induced voltages are in quadrature.

There are, however, also limitations to detuning as the only means of beam-loading compensation. One is known as Robinson's stability criterion [6]. If the amount of detuning calculated by Eq. (30) becomes comparable to the revolution frequency of the particles in a synchrotron, the beam will become unstable. Another one is the finite time of, say, a second, which is needed for the tuner to react. Actually, the time scale of the cavity voltage transients, which may cause beam instabilities, is much shorter. The cavity filling time τ_{CAV} is given by

$$\tau_{\mathrm{CAV}} = 2Q_{\mathrm{L}} / \omega_{\mathrm{CAV}} \ . \tag{34}$$

The cavity voltage rise after injection of a bunched beam with a current $\vec{I}_{\mathrm{B}}(\omega_{\mathrm{CAV}})$ can be approximated by

$$\vec{U}_{\mathrm{B}} \approx R_{\mathrm{SL}} \vec{I}_{\mathrm{B}} \left(1 - e^{-t/\tau}\right) \ . \tag{35}$$

This voltage will add to the cavity voltage produced by the generator, and after a time $t \approx 3\tau$ the total cavity voltage becomes

$$\left|\vec{U}_{\mathrm{CAV}}\right| \approx R_{\mathrm{SL}} \sqrt{\left|\vec{I}_{\mathrm{g}}\right|^2 + \left|\vec{I}_{\mathrm{B}}\right|^2} \tag{36}$$

with a phase shift given by Eq. (30).

Since typical values of τ are below 100 µs and therefore much smaller than the proton synchrotron frequency in a storage ring (T_{S} is usually ≥ several ms), these transients will, in general, excite synchrotron oscillations of the beam with the consequence of emittance blow-up and particle loss. Additional compensation of transient beam loading is therefore necessary. This will be discussed in the following paragraphs.

In Fig. 2 a diagram of a tuner regulation circuit is shown. The phase detector measures the relative phase between generator current and cavity voltage which depends, according to Eq. (20), on the frequency $\Delta\omega$, by which the cavity is detuned. The phase detector output signal acts on a motor that drives a plunger tuner into the cavity volume until there is resonance. An alternative tuner could be a resonant circuit loaded with ferrites. The magnetic permeability μ of the ferrites and hence the resonance frequency of the circuit can be controlled by a magnetic field. This latter method is especially useful when a large tuning range in combination with a low cavity Q is required.

If proper tuner action is necessary in a large dynamic range of cavity voltages, limiters with a minimum phase shift per dB compression have to be installed at the phase detector input. Since this phase shift is decreasing with frequency, all signals should be mixed down to a sufficiently low intermediate frequency.

The signal proportional to the generator current $\vec{I}_{\mathrm{forw.}}$ can be obtained from a directional coupler. In case the RF amplifier is so closely coupled to the cavity that no directional coupler can be installed, the relative phase between RF amplifier input and output signal can also be used to derive a tuner signal [7].

4. REDUCTION OF TRANSIENT BEAM LOADING BY FAST FEEDBACK

The principle of a fast feedback circuit is illustrated in Fig. 2. A small fraction α of the cavity RF signal is fed back to the RF preamplifier input and combined with the generator signal. The total delay δ in the feedback path is such that both signals have opposite phase at the cavity resonance frequency ω_{CAV}. For other frequencies there is a phase shift

$$\Delta\phi = \Delta\omega\delta\,. \tag{37}$$

Therefore the voltage at the amplifier input is now given by

$$\vec{U}'_{\mathrm{in}} = \vec{U}_{\mathrm{in}} - e^{-i\Delta\omega\delta}\alpha\vec{U}_{\mathrm{CAV}}\,. \tag{38}$$

With the voltage gain K of the amplifier we can rewrite Eq. (20) and obtain for the cavity voltage with feedback

$$\vec{U}_{\mathrm{CAV}} \approx \frac{K\left[\vec{U}_{\mathrm{in}} - e^{-i\Delta\omega\delta}\alpha\vec{U}_{\mathrm{CAV}}\right] - \vec{U}_{\mathrm{B}}}{1 + iQ_{\mathrm{L}}2\dfrac{\Delta\omega}{\omega_{\mathrm{CAV}}}} \tag{39}$$

or

$$\vec{U}_{\mathrm{CAV}} \approx \frac{K\vec{U}_{\mathrm{in}} - \vec{U}_{\mathrm{B}}}{1 + iQ_{\mathrm{L}}2\dfrac{\Delta\omega}{\omega_{\mathrm{CAV}}} + e^{-i\Delta\omega\delta}\alpha K}\,. \tag{40}$$

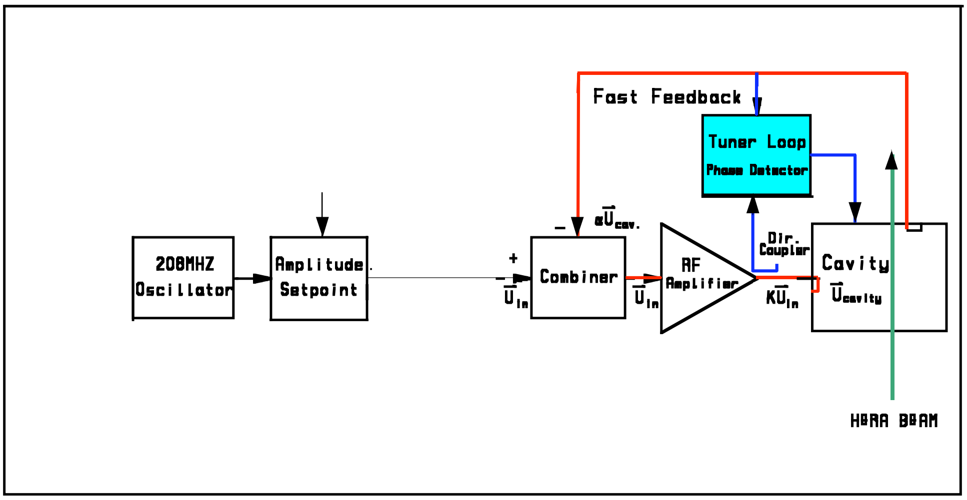

Fig. 2: Schematic of servo loops for phase and amplitude control of the HERA 208 MHz proton RF system

For $\Delta\omega = 0$ and $A_{\mathrm{F}} \gg 1$ this reduces to

$$\vec{U}_{\mathrm{CAV}} \approx \frac{\vec{U}_{\mathrm{in}}}{\alpha} - \frac{\vec{U}_{\mathrm{B}}}{\alpha K}\,. \tag{41}$$

The open loop feedback gain A_F is defined as

$$A_F = \alpha K . \tag{42}$$

One sees that there is a reduction of the beam-induced cavity voltage by the factor $1/A_F$ due to the feedback. This is equivalent to a similar reduction of the cavity shunt impedance as seen by the beam.

$$Z_L \approx \frac{R_{SL}}{1 + iQ_L 2\frac{\Delta\omega}{\omega_{CAV}}} \rightarrow \frac{R_{SL}}{1 + iQ_L 2\frac{\Delta\omega}{\omega_{CAV}} + A_F e^{-i\Delta\omega\delta}} . \tag{43}$$

The price for this fast reduction of beam loading is the additional amount of generator current $\vec{I}_B N$ that is needed almost to compensate the beam current in the cavity. In terms of additional transmitter power P' this reads

$$P' = R_S \hat{\vec{I}}_B^2 / 8. \tag{44}$$

It is the power already calculated by Eq. (32). As there is no change in cavity voltage due to P' this power will be reflected back to the generator, which has to have a sufficiently large plate dissipation power capability. Otherwise a circulator is needed. This critical situation of additional RF power consumption and reflection lasts, however, only until the tuner has reacted, and it may be minimized by pre-detuning. The generator-induced voltage is, of course, also reduced by the amount $1/A_F$, but this can be easily compensated on the low power level by increasing $\vec{U}_{in}$ by the factor $1/\alpha$ as Eq. (41) suggests. The practical implications of this will be illustrated by the following example.

Let the power gain of the amplifier be 80 dB. For a cavity power of 50 kW an input power P_{IN} of 0.5 mW is thus required. This corresponds to a voltage gain of 10^4 so, for a design value of $A_F = 100$, α becomes 10^{-2}. Hence the power that is fed back to the amplifier input, is 5 W. In order to maintain the same cavity voltage as without feedback, P_{IN} has to be increased from 0.5 mW to 5.0005 W. This value can, of course, be reduced by decreasing α. But then the amplifier gain has to be increased to keep A_F constant. This leads to power levels in the 100 µW range at the amplifier input. All this is still practical, but some precautions, such as extremely good shielding and suppression of generator and cavity harmonics, have to be taken.

The maximum feedback gain that can be obtained is limited by the aforementioned delay time δ of a signal propagating around the loop. According to Nyquist's criterion, the system will start to oscillate if the phase shift between $\vec{U}_{in}$ and $\alpha\vec{U}_{CAV}$ exceeds $\approx 135°$. A cavity with high Q can produce a ±90° phase shift even for very small $\Delta\omega$. Therefore, once the additional phase shift given by Eq. (37) has reached $\pm \pi/4$, the loop gain must have become ≤ 1, i.e.

$$|A_F(\Delta\omega_{max})| \approx \frac{\alpha K}{1 + iQ_L 2\frac{\Delta\omega_{max}}{\omega_{CAV}}} \leq 1 \tag{45}$$

where

$$\delta\Delta\omega_{max} = \pm\frac{\pi}{4} . \tag{46}$$

Here we assume that all other frequency-dependent phase shifts, like the ones produced by the amplifiers, can be neglected. Taking $\vec{U}_B = 0$ and inserting Eq. (45) we can solve Eq. (39) for A_F:

$$A_F = \frac{Q_L}{4 f_{CAV}\delta} . \tag{47}$$

This is the maximum possible feedback gain for a given δ.

A fast feedback loop of gain 100 has been realized at the HERA 208 MHz proton RF system. With a loaded cavity Q_L of ≈ 27000 the maximum tolerable delay, including all amplifier stages and cables, is $\delta = 330$ ns. Therefore all RF amplifiers have been installed very close to the cavities in the HERA tunnel.

In addition, there are independent slow phase and amplitude regulation units for each cavity with still higher gain in the region of the synchrotron frequencies, i.e. below 300 Hz. Without fast feedback these units might become unstable at heavy beam loading [8, 9] since changes in cavity voltage and phase are then correlated, as shown by Eqs. (30) and (36).

The effect of a fast feedback loop is revealed in Fig. 3, where the transient behaviour of the imaginary (upper curve) and real (middle curve) part of a HERA 208 MHz cavity voltage vector is displayed. The lower curve is the signal of a beam current monitor, which shows nicely the bunch structure of the beam and a 2 μs gap between batches of 6 × 10 bunches each. A detailed description of this measurement and of the IQ detector used is given in Ref. [10]. In this particular case the upper curve is essentially equivalent to the phase change of the cavity voltage due to transient beam loading, and the middle curve corresponds to the change in amplitude.

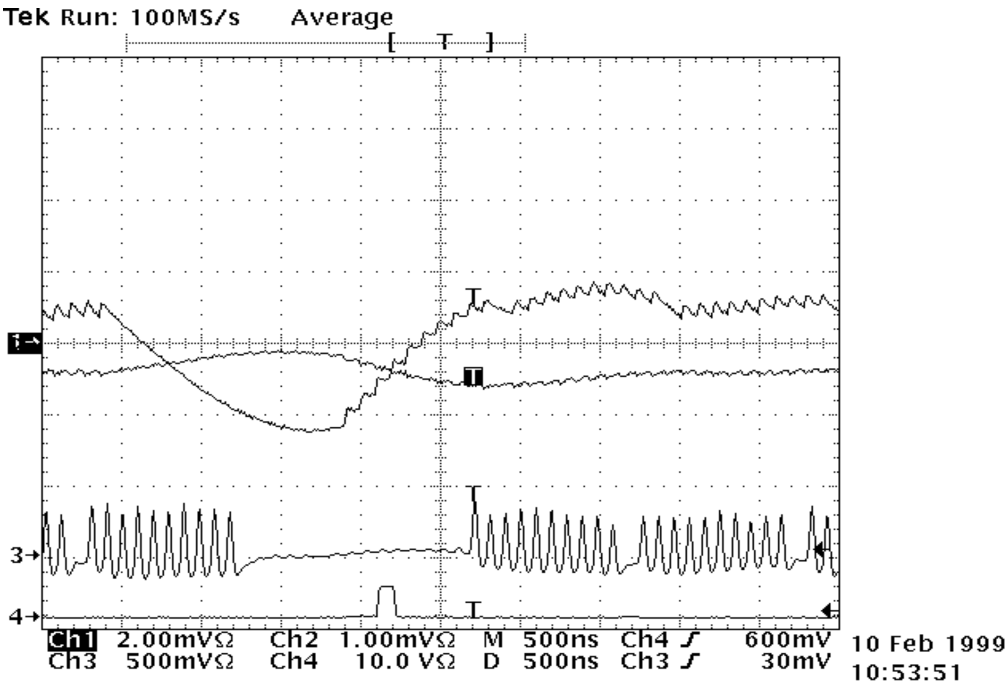

Fig. 3: Transient behaviour of the cavity voltage under the influence of fast feedback. This figure is taken from Ref. [10].

The apparent time shift between the bunch signals and the cavity signals is due to the time of flight of the protons between the location of the cavity and the beam monitor in HERA. The transients resulting from the first two or three bunches after the gap cause step-like transients, which accumulate without significant correction. Later the fast feedback delivers a correction signal, which causes the subsequent transients to look more and more saw-tooth-like. From this one can estimate the time delay in the feedback loop to be of the order of 250 ns. After about 1 μs equilibrium with the beam is reached. Similarly, one observes in the left part of the picture that the feedback correction is still present for 250 ns after the last bunch before the gap has left the cavity. The equilibrium without beam is also reached after about 1 μs. Without fast feedback the time taken to reach equilibrium is about 100 times longer, as one would expect for a feedback gain of 100.

To summarize this Section we state that fast feedback reduces the resonant cavity impedance as seen by an external observer (usually the beam) by the factor $1/A_F$. It is important to realize that any noise originating from sources other than the generator, especially amplitude and phase noise from the amplifiers, will be reduced by the factor $1/A_F$ because the cavity signal is directly compared to the generator signal at the amplifier input stage. Care has to be taken that no noise be created, by diode limiters or other non-linear elements, in the path where the cavity signal is fed back to the amplifier input. This noise would be added to the cavity signal by the feedback circuit.

5. FEEDBACK AND FEEDFORWARD APPLIED TO SUPERCONDUCTING CAVITIES

So far, we have only considered normally conducting cavities in a proton storage ring, where the protons arrive in the cavities at the zero crossing of the RF signal, i.e. at $\phi_s = 0^\circ$ or a few degrees.

In the following I would like to present an example of the other extreme: superconducting cavities in a linear electron accelerator where the electrons cross the cavities near the moment of maximum RF voltage, i.e. at $\phi_s \approx 90^\circ$. (Note that for linear colliders a different definition of ϕ_s is usually used, namely $\phi_s = 0^\circ$ when the particle is on crest. In this article we do not adopt this definition.)

A test facility for TESLA is currently being built at DESY. We refer to the special example of the TESLA Test Facility cavities, which are 9-cell cavities made of pure niobium. The operating frequency is 1.3 GHz.

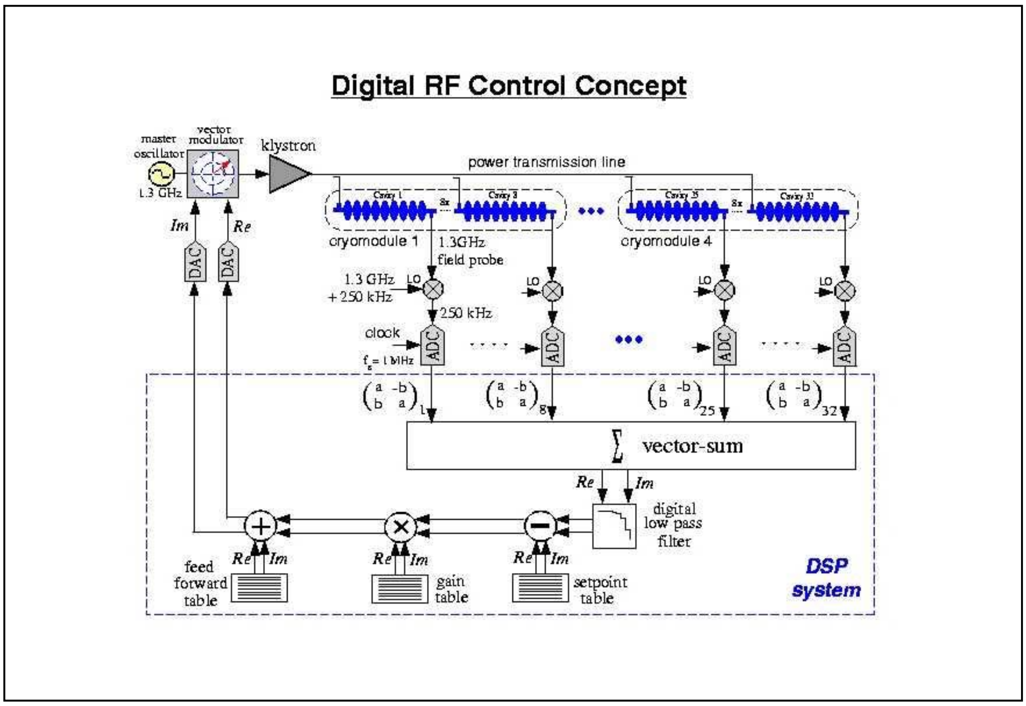

Fig. 4: Schematic of the low-level RF system for control of the TESLA Test Facility 1.3 GHz cavities. This figure is taken from Ref. [11].

The unloaded Q-value of these cavities is in the range 10^9–10^{10}, or even higher. Hence the bandwidth is only of the order of 1 Hz, and also the shunt impedance of these cavities exceeds that of normally conducting cavities by many orders of magnitude. Therefore, we have a coupling factor $\beta \approx 1000$ in this case, which also reflects the fact that the ratio of the power taken away by the beam to the power dissipated in the cavity walls is much larger for superconducting cavities than for normally conducting ones. Owing to the coupling, the nominal loaded Q-value is only 3×10^6, and the loaded cavity bandwidth seen by the beam is 433 Hz. Since in this case there is a circulator with a load to protect the klystron from reflected power, this loaded bandwidth is also seen by the RF generator, which is a klystron. Since the particles are (almost) on crest, only the real part of the admittance [Eq. (27)] seen by the generator is changed due to beam loading. This means that in this example beam loading causes a change only in the cavity impedance seen by the generator and detuning plays no role as a means of beam-loading compensation. Therefore there is only perfect matching for the nominal beam current to which the cavity power input coupler has been adjusted.

From the circuit diagram in Fig. 4 we see that one RF generator is planned to supply up to 32 cavities with RF power. The RF power that is needed per cavity to accelerate an electron beam of 8.5 mA to 25 MeV, is close to 215 kW, hence a klystron power close to 7 MW is needed. This power is entirely carried away by the beam. In contrast to the previous example, where all the RF power was essentially dissipated in the normally conducting cavity walls, the power needed to build up the RF cavity voltage in the superconducting cavities is only a few hundred watts. A high-efficiency, 10 MW, multibeam klystron has been developed for this project. For completeness we mention that this is pulsed power, with a pulse length of 1.5 ms and a maximum repetition rate of 10 Hz. So the maximum average klystron power is 150 kW.

The RF seen by the beam corresponds to the vector sum of all cavity signals. Therefore for the RF control system such a vector sum needs to be generated. This is done by down conversion of the cavity signals to 250 kHz intermediate frequency signals that are sampled in time steps of 1 μs. Each set of two subsequent samples corresponds to the real and imaginary part of the cavity voltage vector. The vector sum is generated in a computer and is compared to a table of set point values. The difference signal, which corresponds to the cavity voltage error, acts on a vector modulator at the low-level klystron input signal. In addition to this feedback a feedforward correction can be added. The advantage of feedforward is that, in principle, there is no gain limitation as in the case of feedback. If the error is known in advance, one can program a counteraction in the feedforward table. Examples of such errors could be a systematic decrease in beam current during the pulse due to some property of the electron source, or a systematic change in the cavity resonance frequency during the pulse. This effect does indeed exist. The mechanical forces resulting from the strong pulsed RF field in the superconducting cavities cause a detuning of the order of a few hundred hertz at 25 MV/m. This effect is called Lorentz force detuning.

From Eq. (47) one might infer that, because of the large value of Q_L, the maximum possible feedback gain in this case could become significantly larger than for normally conducting cavities. However, one has to check whether there are poles in the system at other frequencies, and, at least in this case, there is a fairly large loop delay of about 4 μs caused by the 12 m length of the cryogenic modules in which the cavities are placed and by the time delay in the computer. This results in a realistic maximum loop gain of 140.

So far, we have demonstrated for up to 16 cavities that all this really does work in practice. The impressive phase and amplitude stability of 0.1 degree and 0.5% that has been reached with this feedback system is shown in Fig. 5. There one also sees that the addition of feedforward improves the amplitude and phase stability to 0.05% and 0.03 degrees respectively.

6. DAMPING OF SYNCHROTRON OSCILLATIONS OF PROTONS IN THE PETRA II MACHINE

In the preceding sections phase and amplitude control of the cavity voltage was discussed. In this last Section we would like to give an example of beam control by looking at the dedicated RF system for the damping of synchrotron oscillations of protons in the PETRA II synchrotron at DESY.

Prior to injection into HERA, protons are pre-accelerated to 7.5 and 40 GeV/c in the DESY III and PETRA II synchrotrons, respectively [13]. Timing imperfections during the transfer of protons from one machine to the next and RF noise during ramping were observed to cause synchrotron oscillations that, if not damped properly, may lead to an increase in beam emittance and to significant beam losses. Therefore a phase loop acting on the RF phase to damp these oscillations of the proton bunches is a necessary component of the low-level RF system. The PETRA II proton RF system, which consists of two 52 MHz cavities, each with a closely coupled RF amplifier chain and a fast feedback loop of gain 50, is similar to the one shown in Fig. 2. The block diagram of the PETRA II phase loop, on which I shall now concentrate, is shown in Fig. 6.

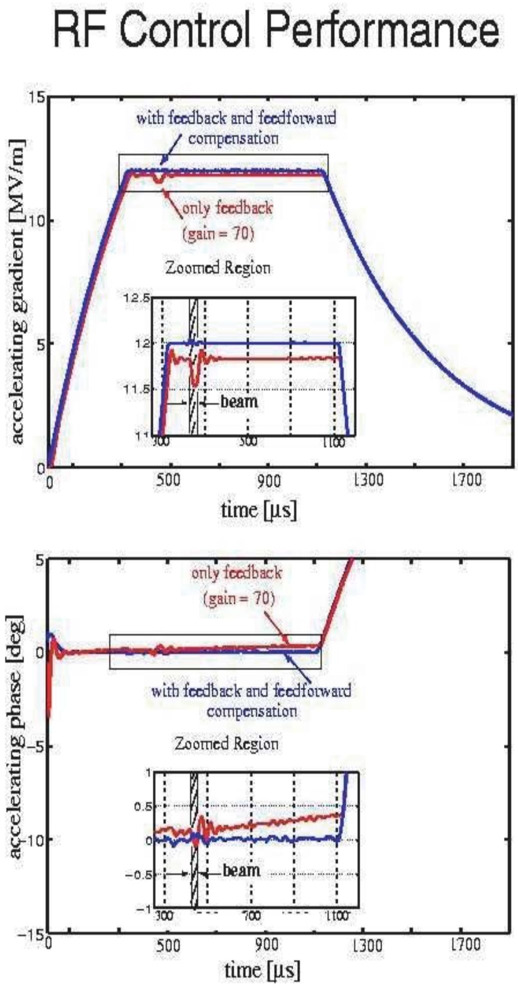

Fig. 5: Phase and amplitude stability achieved by digital feedback and feedforward in a 1.3 GHz cavity of the TESLA Test Facility. The obtained phase and amplitude stability with feedback alone is 0.5% and 0.1 degrees. With feedforward an improvement to 0.05% and 0.03 degrees was reached. This figure is taken from Ref. [12].

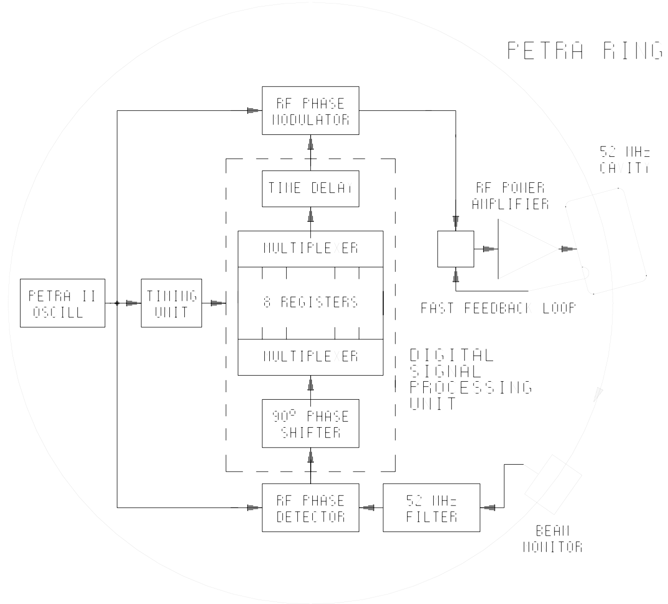

Fig. 6: Block diagram of the PETRA II phase loop. In the phase detector, synchrotron oscillations of the bunches are detected by comparing the filtered 52 MHz component of the beam with the 52 MHz RF reference source. An average phase signal for each of the eight batches of ten bunches is phase shifted by 90° with respect to the synchrotron frequency, stored in its register, and properly multiplexed to the phase modulator acting on the RF drive signal.

6.1 Loop bandwidth

The maximum number of bunches is 11 in DESY III and 80 in PETRA II, so eight DESY III cycles are needed to fill PETRA II. If synchrotron oscillations arise due to injection timing errors, all bunches of the corresponding batch are expected to oscillate coherently. Therefore one single correction signal can damp the bunch oscillations in that batch and in total up to eight such signals are needed, one for each batch. This phase loop is a batch-to-batch rather than a bunch-to-bunch feedback. Ideally, the correction of expected errors of about two degrees in the injection phase has to be switched within the 96 ns separating the last bunch of batch n from the first bunch of batch $n + 1$. Owing to the fast feedback of gain 50, the RF system has an effective bandwidth of about 1 MHz. However, it is capable of performing small phase changes of the order of 1° per 100 ns, which should be sufficient for damping synchrotron oscillations also in the multibatch mode of operation.

6.2 The phase detector

Each bunch passage generates a signal in the inductive beam monitor, also shown in Fig. 6. A passive LC filter of 8 MHz bandwidth filters out the 52 MHz component. The ringing time is comparable to the bunch spacing time as shown in Fig. 7. Amplitude fluctuations of this signal are reduced to ±0.5 dB in a limiter of 40 dB dynamic range. So the amplitude dependence of the synchrotron phase measurement between the bunch signal and the 52 MHz RF source signal is minimized. The phase detector has a sensitivity of 10 mV per degree. By inserting a low pass filter one can directly observe the synchrotron motion of the bunches at the phase detector output. This is shown in Fig. 8(a) for one batch of nine proton bunches circulating in PETRA II with a momentum of 7.5 GeV/c a few milliseconds after injection. The observed synchrotron period $T_S = 5$ ms agrees with the expected value for the actual RF voltage of 50 kV.

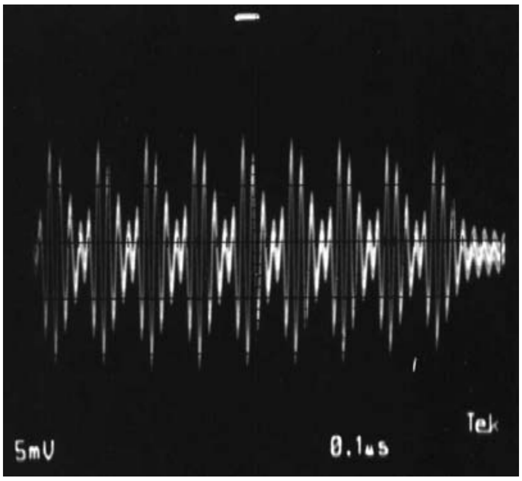

Fig. 7: Filtered signal of a batch of nine proton bunches circulating in PETRA. The bunch spacing time is 96 ns.

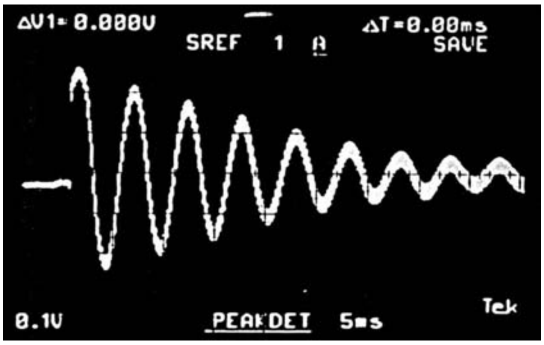

Fig. 8(a): The synchrotron oscillation measured at the phase detector output a few milliseconds after injection of a batch of nine proton bunches into PETRA II. It is smeared out by Landau damping after several periods. The damping loop is not active.

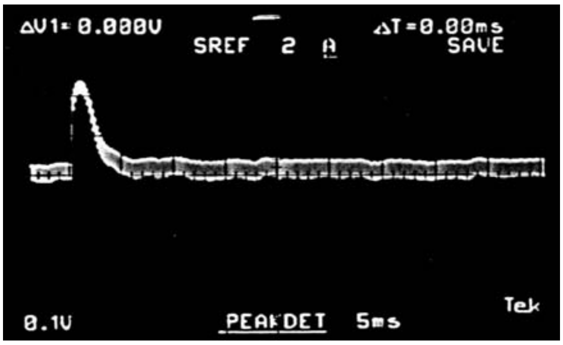

Fig. 8(b): Same as Fig. 8(a) but with the phase loop active. The synchrotron oscillation is completely damped within half a synchrotron period of 5 ms.

6.3 The FIR filter as a digital phase shifter

A feedback loop can damp the synchrotron motion if, as is indicated in Fig. 6, the synchrotron phase signal is shifted by –90° relative to the synchrotron frequency f_S, delayed properly, and fed into a phase modulator acting on the 52 MHz drive signal. The necessity of the –90° phase shift relative to f_S can be seen from the equation of damped harmonic motion $\ddot{x} + a\dot{x} + bx = 0$ with the solution $x = A\sin(\omega_S t - \phi)e^{-at}$. The damping term $a\dot{x}$ is proportional to the time derivative of the solution x, i.e. a phase shift of –90°. The correction signal will coincide with the corresponding batch in the cavity if the total delay $\delta = t_f + nT_{rev}$, where t_f is the transit time from the beam monitor to the cavity, n an integer, and T_{rev} = 7.7 µs is the particle revolution time in PETRA. Since $T_S \gg T_{rev}$, a delay even of more than one turn ($n > 1$) would not be critical.

Rather than using a simple RC integrator of differentiator network as a 90° phase shifter, which is not without problems [14], a more complex digital solution with a software controlled phase shift has been adopted. This is very attractive since during injection, acceleration, and compression of the bunches the synchrotron frequency varies in the range from 200 Hz to 350 Hz. In addition, storing and multiplexing the eight correction signals for each of the eight possible batches in PETRA II can also be realized most comfortably on the digital side. The phase shifter has been built up as a three-coefficient digital Finite-length Impulse Response (FIR) filter according to

$$g_\mu = \sum_{k=0}^{2} h_k f_{\mu-k} \tag{52}$$

with an amplitude response

$$H(\omega) = \sum_{k=0}^{2} h_k e^{-ik\omega T_S} \quad , \tag{53}$$

where f and g are input and output data respectively. Using the coefficients $h_0 = \frac{2}{\pi}\sin\phi$, $h_1 = \cos\phi$, $h_2 = -\frac{2}{\pi}\sin\phi$ one obtains a phase shift that, in the frequency range of interest 200 Hz $\le f_S \le$ 359 Hz, deviates by less than ±0.4 from the nominal value $\phi = -\pi/2$ in accordance with Eqs. (52) and (53). The frequency dependence of the phase shift is mainly due to the delay in the filter, which is of the order of 1 ms, i.e. two sampling periods. It can always be corrected by software, if necessary. The amplitude response is constant within a few per cent for all frequencies.

A block diagram of the filter is shown in Fig. 9. The synchrotron phase information of the eight batches is sampled at intervals T_S = 0.5 ms and passed through eight times three shift registers. The three coefficients are stored in ROMs and are appropriately combined with the phase information. So the first filter output is available after three sampling periods and is then renewed every 0.5 ms.

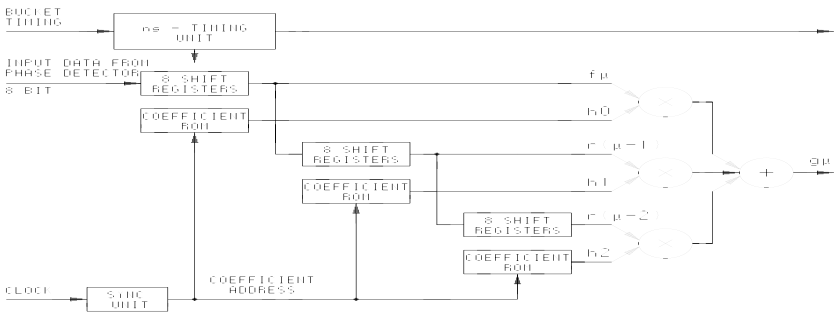

Fig. 9: Block diagram of the FIR filter. From three successive sampling periods the averaged phase signals for the eight proton batches in PETRA II are stored in shift registers and combined with the three coefficients, which are stored in ROMs. The first phase-shifted output is available after three sampling periods of 0.5 ms and is renewed every sampling period.

6.4 Performance of the phase loop

The performance of the loop is demonstrated in Fig. 8, where the phase detector output recorded by a storage scope is displayed. Complete damping of the synchrotron oscillation is achieved within less than one period. This corresponds to a damping time of less than 4 ms. If the loop is operated in the antidamping mode, the beam is lost within some milliseconds. With the loop, losses of the proton beam in PETRA II during energy ramping could be significantly reduced.

REFERENCES

[1] R.E. Collin, *Foundations for Microwave Engineering* (McGraw-Hill, New York, 1966).

[2] P.B. Wilson, CERN ISR–TH/7823 (1978).

[3] D. Boussard, CERN, SPS/86–10 (ARF) (1986).

[4] R.D. Kohaupt, ‘Dynamik intensiver Teilchenstrahlen in Speicherringen’, Lecture Notes, DESY (1987).

[5] A. Piwinski, DESY H 70/21 (1970).

[6] K.W. Robinson, CEA Report CEAL-1010 (1964).

[7] F. Pedersen, *IEEE Trans. Nucl. Sci.* **NS 32** (1985) 2138.

[8] D. Boussard, CERN SPS/85–31 (ARF) (1985).

[9] F. Pedersen, *IEEE Trans. Nucl. Sci.* **NS 22** (1975) 1906.

[10] E. Vogel, ‘Ingredients for an RF Feedforward at HERA’, DESY HERA 99–04 (1999) p. 398.

[11] S. Simrock, private communication, DESY (1999).

[12] M. Liepe, Diploma Thesis, DESY (2000).

[13] A. Gamp, W. Ebeling, W. Funk, J.R. Maidment, G.H. Rees, C.W. Planner, *in* Proc. 1st European Particle Accelerator Conference (EPAC 1), Rome, 1988, Ed. S. Tazzari (World Scientific, Singapore, 1989).

[14] A. Gamp, *in* Proc. 2nd European Particle Accelerator Conference (EPAC2), Nice, 1990, Eds. P. Marin and P. Mandrillong (Ed. Frontières, Gif-sur-Yvette, 1990).